# Structural Insights into (Tere)phthalate-Ester Hydrolysis by a Carboxylesterase and Its Role in Promoting PET Depolymerization

Gerlis von Haugwitz, Xu Han, Lara Pfaff, Qian Li, Hongli Wei, Jian Gao, Karen Methling, Yufei Ao, Yannik Brack, Jan Mican, Christian G. Feiler, Manfred S. Weiss, David Bednar, Gottfried J. Palm, Michael Lalk, Michael Lammers, Jiri Damborsky, Gert Weber, Weidong Liu,* Uwe T. Bornscheuer,* and Ren Wei*

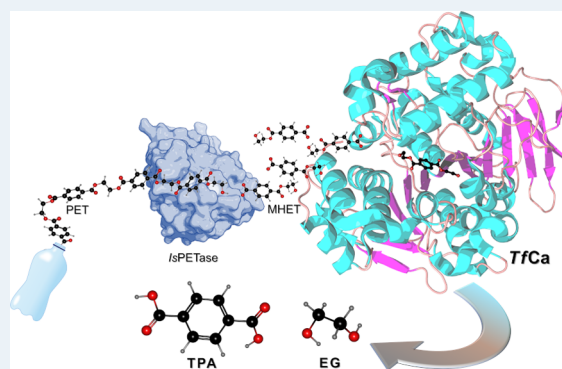Cite This: *ACS Catal.* 2022, 12, 15259−15270

Read Online

ACCESS | Metrics & More | Article Recommendations | Supporting Information

**ABSTRACT:** TfCa, a promiscuous carboxylesterase from *Thermobifida fusca*, was found to hydrolyze polyethylene terephthalate (PET) degradation intermediates such as bis(2-hydroxyethyl) terephthalate (BHET) and mono-(2-hydroxyethyl)-terephthalate (MHET). In this study, we elucidated the structures of TfCa in its apo form, as well as in complex with a PET monomer analogue and with BHET. The structure–function relationship of TfCa was investigated by comparing its hydrolytic activity on various ortho- and para-phthalate esters of different lengths. Structure-guided rational engineering of amino acid residues in the substrate-binding pocket resulted in the TfCa variant I69W/V376A (WA), which showed 2.6-fold and 3.3-fold higher hydrolytic activity on MHET and BHET, respectively, than the wild-type enzyme. TfCa or its WA variant was mixed with a mesophilic PET depolymerizing enzyme variant [*Ideonella sakaiensis* PETase (*Is*PETase) PM] to degrade PET substrates of various crystallinity. The dual enzyme system with the wild-type TfCa or its WA variant produced up to 11-fold and 14-fold more terephthalate (TPA) than the single *Is*PETase PM, respectively. In comparison to the recently published chimeric fusion protein of *Is*PETase and MHETase, our system requires 10% *Is*PETase and one-fourth of the reaction time to yield the same amount of TPA under similar PET degradation conditions. Our simple dual enzyme system reveals further advantages in terms of cost-effectiveness and catalytic efficiency since it does not require time-consuming and expensive cross-linking and immobilization approaches.

**KEYWORDS:** *PET hydrolysis, plastic, dual enzyme system, carboxylesterase, structure, enzyme engineering*

## INTRODUCTION

In recent years, enzymatic depolymerization of polyethylene terephthalate (PET) has emerged as an alternative technology to conventional mechanical and chemical plastic recycling approaches.[1] TfH from *Thermobifida fusca* (*T. fusca*) was the first enzyme discovered in 2005 to possess PET degrading activity.[2] Since then, many new PET hydrolases (PETases) have been identified and engineered for higher PET degradation efficiency.[3−5] Enzymatic PET hydrolysis produces small-molecule degradation products, which can be recovered and used to synthesize virgin polymers.[5,6] In addition to the desired PET monomers terephthalate (TPA) and ethylene glycol (EG), bis(2-hydroxyethyl) terephthalate (BHET) and mono-(2-hydroxyethyl)-terephthalate (MHET) are also released as degradation intermediates that are known as inhibitors for selected PETases.[7]
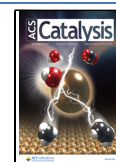
Methods for mitigating the product inhibition during enzymatic PET hydrolysis include the continuous removal of small-molecule products using ultrafiltration membranes,[8] the use of engineered PETase variants that are less affected by the inhibitors,[9] and the introduction of a helper enzyme with a specific hydrolytic activity on the inhibitors. *Ideonella sakaiensis* (*I. sakaiensis*) is a bacterium that can degrade PET and assimilate its monomers.[10] In addition to the extracellular *I. sakaiensis* PETase (*Is*PETase) which can depolymerize PET predominantly to MHET, the intracellular MHETase has been assumed to facilitate the PET assimilation by converting MHET to TPA and EG.[10,11] This allowed for the development of a chimeric MHETase:*Is*PETase fusion protein exhibiting markedly improved PET depolymerization activity.[12] At 30 °C and pH 7.5, this chimeric system produced approximately

sixfold more degradation products in 96 h than single *Is*PETase in the PET hydrolysis. TfCa is a *T. fusca* carboxylesterase with hydrolytic activity on PET oligomers, including MHET, BHET, and a cyclic PET trimer.[13,14] When TfCa was immobilized on a SulfoLink resin and then coupled with various PETases such as LC-cutinase or TfCut2 for PET degradation, the yield of degradation products was up to twofold higher than when TfCa was absent.[15] Nevertheless, both dual enzyme systems may be less feasible for industrial applications due to the need of an efficient cross-linking method or the high cost of the immobilization matrix. Therefore, a low-cost dual enzyme system with enhanced PET oligomer hydrolyzing activity is required.

While the crystal structures of MHETase have been recently solved and repeatedly reported,[11,12,16] the structural basis underlying the mechanism of TfCa-catalyzed hydrolysis of TPA esters remains elusive. In this study, we elucidated the first crystal structure of TfCa in its apo form and in complex with the MHET-like analogue 4-[(2-hydroxyethyl) carbamoyl] benzoic acid (MHETA) and BHET at atomic resolutions. By comparing its specific activity on various TPA esters and an ortho-phthalate ester (diethyl phthalate, DEP), the structural basis for substrate recognition and hydrolysis by TfCa was explored. Moreover, we rationally engineered TfCa and obtained a mutant with significantly higher MHET and BHET hydrolytic activity. This TfCa variant was applied in a simple dual enzyme system in combination with an *Is*PETase penta-mutant, *Is*PETase$^{S121E/D186H/R280A/N233C/S282C}$ (*Is*PETase PM), for enhanced degradation of a variety of PET substrates with different crystallinity.

## MATERIAL AND METHODS

**Materials.** Chemicals and consumables were purchased from Merck KGaA (Darmstadt, Germany), Sigma-Aldrich (Steinheim, Germany), Thermo Fisher Scientific (Waltham, MA, USA), and New England Biolabs GmbH (Frankfurt am Main, Germany) unless stated otherwise. Primers were ordered from Eurofins (Ebersberg, Germany) and Thermo Fisher Scientific (Waltham, MA, USA). The amorphous PET film (GfPET, ES30-FM-0001445) and the semi-crystalline PET powder (maximum particle size: 300 $\mu$m, crystallinity >40%, product number: ES306031/1) were purchased from Good-fellow GmbH (Bad Nauheim, Germany). PET nanoparticles (PET-NP) were prepared as described previously by Pfaff et al.,[17] bis[2-(benzoyloxy)ethyl] terephthalate was defined as 3PET and synthesized according to Fischer-Colbrie et al.,[18] MHETA was synthesized as described by Palm et al.[11]

**Crystallization, Data Collection, Structure Determination, and Refinement.** All crystallization experiments were conducted at 25 °C using the sitting-drop vapor-diffusion method. In general, 1 $\mu$L TfCa solution (40 mg/mL in 25 mM Tris−HCl containing 150 mM NaCl, pH 7.5) was mixed with 1 $\mu$L reservoir solution in 48-well Cryschem Plates and equilibrated against 100 $\mu$L of the reservoir solution. The optimized crystallization conditions of TfCa and TfCa E319L were 22% (w/v) poly(acrylic acid) sodium salt 5100, 0.02 M MgCl$_2$, 0.1 M HEPES at pH 7.5. The mutant TfCa E319L was created to eliminate residue E319 of the catalytic triad to avoid the hydrolysis of the substrate during the soaking period. A detailed description of the enzyme expression for crystallization purposes is included in the Supporting Information.

Within 5−6 days, the crystals reached their final size suitable for X-ray diffraction. The TfCa and TfCa E319L crystals in complex with MHETA, BHET, or MHET plus BHET were obtained by soaking the enzyme with 10 mM of each compound for 72 h.

All the X-ray diffraction data sets were collected at the National Facility for Protein Science in Shanghai at Shanghai Synchrotron Radiation Facility at the beamlines BL10U2/BL02U1(BL17U)/BL17B/BL18U1/BL19U1, and in Berlin at the third-generation synchrotron radiation source (BESSY II) with beamline 14.1.[19] The crystals were mounted in a cryoloop and soaked with cryoprotectant solution [25% (w/v) poly-(acrylic acid sodium salt) 5100, 0.02 M MgCl$_2$, 0.1 M HEPES pH 7.5, 10% glycerol] prior to data collection at 100 K. The diffraction images were processed using HKL2000. The crystal structure of TfCa was solved by the molecular replacement method with the Phaser program[20] from the Phenix[21] suite using the structure of the carboxylesterase from *Geobacillus stearothermophilus* (PDB-ID: 2OGT) as a search model. Further refinement was carried out using the programs phenix.refine[22] and Coot.[23] Prior to structural refinement, 5% of randomly selected reflections were used for calculating $R_{\text{free}}$[24] to monitor the refinement process. Data collection and refinement statistics are summarized in Table S1.

**Expression and Purification of Recombinant TfCa and *Is*PETase PM.** For enzymatic PET degradation, the TfCa gene was cloned into a pET20b(+) vector and the plasmid was transformed into *Escherichia coli* BL21 (DE3). Bacterial cells were grown in lysogeny broth (LB) medium at 37 °C to an optical density at 600 nm (OD$_{600}$) of 1 and then further incubated at 18 °C. When the OD$_{600}$ reached 1.5, recombinant protein expression was induced by adding 1 mM isopropyl $\beta$-D-thiogalactopyranoside and cells were further grown at 18 °C until an OD$_{600}$ of 3. Cells were harvested by centrifugation at 10,000 × $g$ for 5 min. Cell pellets were re-suspended in lysis buffer containing 50 mM Na$_2$HPO$_4$ (pH 8) and 150 mM NaCl, followed by disruption by ultrasonication (3 × 90 s, 50% pulse, 50% power, 2 min breaks). Cell debris was removed by centrifugation at 10,000 × $g$ for 30 min. The supernatant was then applied to a Ni$^{2+}$-nitrilotriacetic acid column, washed with lysis buffer and a 20−90 mM imidazole gradient as described before.[14] The enzyme with an apparent molecular mass of 55 kDa was eluted with 250 mM imidazole, which was then exchanged to the assay buffer (25 mM Tris−HCl, pH 7.5, set at 45 °C) using Vivaspin (Sartorius Lab Instruments, Göttingen, Germany) with 10 kDa cutoff. The membrane of the Vivaspin was equilibrated with 5 mL Tris−HCl buffer (25 mM, pH 7.5, set at 45 °C) by centrifugation for 5 min at 5000 × $g$. Afterward, the eluted protein was added to the Vivaspin, topped with 5 mL Tris−HCl buffer, and centrifuged for 15 min at 5000 × $g$ and 4 °C. After repeating this four times, the enzyme was removed from the upper compartment of the Vivaspin column. The enzyme concentration was determined using a NanoDrop 1000 device (Thermo Fisher Scientific, Waltham, MA, USA). *Is*PETase PM was expressed as described by Brott et al.[25] and purified as described here for TfCa. The model substrate para-nitrophenyl acetate (pNPA) was used for determining the enzymatic activity as described before.[14]

**Site-Directed Mutagenesis.** Mutation of the TfCa-encoding gene was performed using the Q5 Site-Directed Mutagenesis Kit (New England Biolabs GmbH, Frankfurt am Main, Germany) according to the supplier's protocol. Successful mutagenesis was confirmed by sequencing.

**Enzymatic Production of the Substrate MHET.** Similar to terephthalic acid, commercially available MHET has a

benzoic acid end group and is hence almost insoluble in aqueous solutions without organic solvents. Therefore, soluble MHET with a deprotonated carboxylate end was prepared from controlled enzymatic BHET degradation using TfCa as described earlier.[7] Up to 100 mM BHET was added into ethanol and sonicated in a water bath for 30 min until BHET was dissolved to form a clear solution. The production of MHET was carried out in a 50 mL reaction volume, containing 20 mM of BHET in ethanol, 550 nM of purified TfCa, and 25 mM Tris−HCl buffer (pH 7.5, set at 45 °C). The final concentration of ethanol in the reaction was 10%. The solution was incubated at room temperature for 30 min without agitation. After incubation, the sample was heated to 80 °C for 10 min to inactivate TfCa and then centrifuged ($10,000 \times g$, 5 min) to remove insoluble compounds. The supernatant was analyzed using high-performance liquid chromatography (HPLC) to ensure MHET purity and then used as a substrate for further enzyme characterization.

**Enzymatic Hydrolysis of Various Substrates.** Enzymatic hydrolysis of the small ester substrates 3PET, BHET, MHET, and DEP was performed in 1 mL reaction volume using 25 mM Tris−HCl buffer (pH 7.5) at 50 °C with 550 nM purified enzyme unless stated otherwise. In total, 2 mM 3PET, BHET, or MHET, or 5 mM DEP were used in the reactions. For an enhanced solubility of the substrates, the hydrolysis of 3PET, BHET, and MHET was performed in the presence of 10% ethanol and that of DEP hydrolysis in 10% dimethyl sulfoxide. Sampling at different time points during hydrolysis reactions was performed as indicated below in the Results section. The degradation products benzoic acid (BA), BHET, MHET, and TPA were confirmed by HPLC, whereas monoethyl phthalate (MEP) was confirmed by liquid chromatography coupled with mass spectrometry (LC−MS). A detailed description of the LC−MS method is included in the Supporting Information.

In a dual enzyme system, PET-NP, PET powder, or PET film were employed as substrates. PET-NP were used at a final concentration of 2, 20, and 200 $\mu$g/mL, whereas PET powder and PET film were used at a final concentration of 60 mg/mL in Tris−HCl buffer (set to pH 7.5 at 45 °C). Purified *Is*PETase PM was used at a concentration of 30 nM for PET-NP and 50 nM for PET film and PET powder as described before.[25] The amounts of the aromatic products were determined using HPLC according to Palm et al.[11] The amount of TPA, MHET, or BHET was calculated based on a TPA standard curve and the amount of MEP was calculated based on a phthalic acid (PA) standard curve. The specific activity was calculated as U/$mg_{enzyme}$, while one unit (U) was defined as one $\mu$mol substrate converted per min.

**Determination of Melting Points.** The melting points ($T_m$) of TfCa and its mutants were determined using nano differential scanning fluorimetry on a Prometheus NT.48 device (NanoTemper Technologies, Munich, Germany). Purified enzymes at a concentration of 300 $\mu$g/mL were used to monitor the thermal denaturation profiles from 40 to 80 °C at 1 °C/min steps. $T_m$ was calculated based on the excitation changes at 285 nm with emission wavelengths at 330 and 350 nm.

**Molecular Docking.** Molecular docking of 3PET, DEP, and MEP into the active site of TfCa was performed with an AutoDock Vina v1.2.0 and Dockprep as part of Chimera v1.15.[26] The docking for 3PET was performed in a box with an edge length of 50 Å around S185, the docking for DEP and MEP was performed in a box with an edge length of 25 Å for DEP and MEP around residue A108, which includes the active site and its surroundings. The AutoDock Vina score was set to −9.9, −6.2, and −6.0 for 3PET, DEP, or MEP, respectively.

**Molecular Dynamics Simulations.** The crystal structures of TfCa with the ligand MHETA (PDB-ID: 7W1J, 1.92 Å) as well as the chain A structure of MHETase from *I. sakaiensis* (PDB-ID: 6QGA, 2.1 Å)[11,27] were used for molecular dynamics (MD) simulations. In total, three independent MD replicates with 20 ns long production simulation were run for each system at 310 K (37 °C) using the Langevin thermostat at a constant pressure of 1.0 bar and a pressure coupling constant of 1.0 ps. Coordinates were saved at intervals of 4 ps. In total, 60 ns of simulation time was produced for each enzyme−ligand system.

Each complex was clustered into three trajectories and the molecular mechanics/generalized Born surface area (MM/GBSA)[28,29] method was applied to calculate the binding free energy ($\Delta G_{bind}$) of MHET in the enzymes and the respective residue-by-residue interactions.[28,30] A more detailed description of these MD simulations is included in the Supporting Information.

## RESULTS

**Structure of TfCa in Its Apo Form.** The ligand-free wild-type TfCa (TfCa wt) was crystallized in the monoclinic space group P2$_1$ (PDB-ID: 7W1K, 1.40 Å). The enzyme is built from three domains, a hydrolase domain that adopts the fold of a canonical $\alpha/\beta$ hydrolase with a central antiparallel $\beta$-sheet surrounded by $\alpha$-helices, a lid domain A and a lid domain B (Figure 1A). As predicted from sequence alignment with homologous enzymes that exhibit carboxylesterase activity, TfCa contains a strictly conserved catalytic triad consisting of the residues S185, E319, and H415. Hence, a *p*-nitrobenzyl esterase (pNB-E) from *Bacillus subtilis* (PDB-ID: 1QE3) and the carboxylesterase Est55 from *G. stearothermophilus* (PDB-ID: 2OGS) were used as templates for elucidating the backbone structure of TfCa. Within the catalytic triad of TfCa, S185 serves as the nucleophile and is located within hydrogen-bond (H-bond) distance to be polarized by the base H415, which is stabilized by the acid E319. A sequence alignment, as well as structural alignments of pNB-E, Est55, and TfCa, are shown in Figures S1 and S2.

**Binding Modes to PET-Related Ligands.** To explore the catalytic mechanism of TfCa, protein crystals were soaked with the substrates MHET and BHET as well as with the substrate analogue MHETA. MHETA has an amide bond in place of the ester bond in MHET and can hence not be hydrolyzed by esterolytic enzymes including TfCa. With TfCa wt, a ligand-bound structure of TfCa with MHETA (PDB-ID: 7W1J, 1.92 Å) was solved. By mutating E319 in the catalytic triad, an inactive TfCa variant E319L was generated. This variant allowed for stable substrate binding and two additional complex structures with BHET (PDB-ID: 7W1L, 2.43 Å) and with both degradation intermediates, MHET and BHET (PDB-ID: 7W1I, 1.67 Å). In the ligand-bound structures of TfCa, the ligands were located at the bottom of a deep active site cleft containing the hydrophobic residues L282, L322, and V376. The side chain of the catalytic S185 is within H-bonding distance to the ester oxygen atom of BHET (PDB-ID: 7W1I, Figure 1E) and the nitrogen atom of MHETA (PDB-ID: 7W1J, Figure 1B).
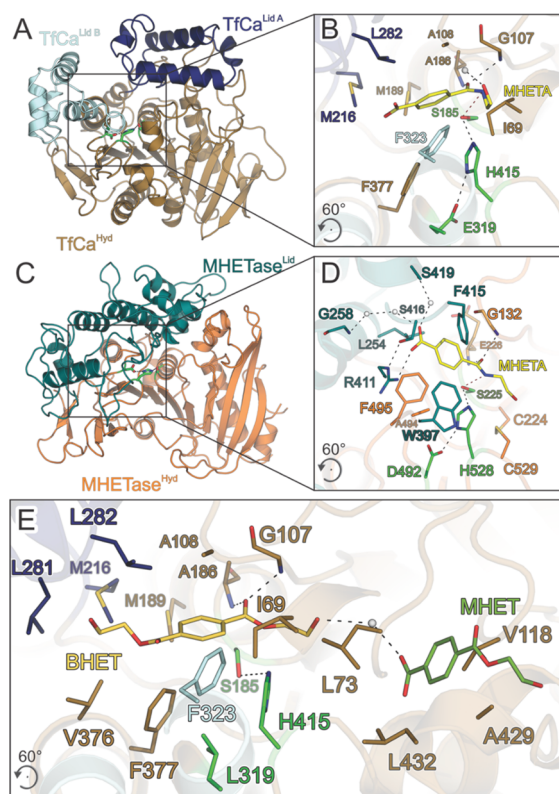
**Figure 1.** Ligand-free and complex structures of TfCa from *T. fusca* in comparison to MHETase from *I. sakaiensis*. (A) Crystallographic structure of TfCa reveals three subdomains: hydrolase domain (TfCa[Hyd], brown), lid domain A (TfCa[LidA], dark blue), and lid domain B (TfCa[LidB], cyan). The catalytic triad consisting of S185, E319, and H415 is shown as green sticks. (B) Close-up view of the active site of TfCa with bound MHETA (yellow) (PDB-ID: 7W1J, 1.92 Å). Residues from different domains are shown in brown (TfCa[Hyd]), dark blue (TfCa[LidA]), and cyan (TfCa[LidB]). (C) Structure of MHETase from *I. sakaiensis* with its two domains: the hydrolase domain (MHETase[Hyd], orange) and the lid domain (MHETase[Lid], dark aquamarine) (PDB-ID: 6QGA).[11] (D) Close-up view of the active site of MHETase with bound MHETA (yellow). Residues from different domains are shown in orange (MHETase[Hyd]) and dark aquamarine (MHETase[Lid]). (E) Close-up view of the active site of TfCa E319L with bound BHET (yellow) and MHET (green) (PDB-ID: 7W1I, 1.67 Å). Dashed lines indicate H-bond formation, molecules and interacting residues are colored by atom types: carbon: varying colors, nitrogen: blue, oxygen: red. Residues of the catalytic triad are shown as green sticks.

The overall structures of TfCa and MHETase and their binding modes to the ligand MHETA are compared as shown in Figure 1A−D. While MHETase consists of one hydrolase domain and one lid domain, the overall structure of TfCa can be divided into one hydrolase domain and two lid domains (Lid A and Lid B). In the active site of TfCa, only three H-bonds are formed, preliminarily with the amide bond and the neighboring hydroxyl end in MHETA (Figure 1B). By comparison, five H-bonds are present in MHETase to interact with both ends of the MHETA ligand (Figure 1D). Side chains of selected phenylalanine residues (F323 and F377 for TfCa, F495 and F415 for MHETase) were found to be potentially involved in stabilizing the TPA moiety in MHETA. In MHETase, F415 and F495 are located on both sides of the benzoic ring of the soaked MHETA ligand. In contrast, F323 and F377 in TfCa are exclusively positioned on one side of

MHETA. This binding mode may only permit a staggered stacking interaction of F323 and a very weak T-shaped interaction of the more distant F377 from the same direction to the TPA moiety (Figure 1B). Similar interactions between these two aromatic residues and the BHET ligand (Figure 1E) suggest that F377 plays a minor role in the substrate stabilization.

We also investigated the binding of MHET to TfCa and MHETase using MD simulations. As shown in Table S5, by clustering the snapshots during the 60 ns productive simulations, MHET has a significantly higher likelihood of staying in the substrate binding pocket of MHETase than in that of TfCa. For clustering the snapshots, the distance between the MHET ester carbonyl atom and the side chain oxygen of the catalytic serine in each enzyme is defined as the catalytic C−O distance. Those snapshots with a catalytic C−O distance less than 4.5 Å were selected to calculate the binding free energy of MHET to individual residues in the substrate binding pocket of each enzyme using MM/GBSA.[29] In MHETase we found that, in addition to the aforementioned F415 and F495, R411 and W397 considerably contribute to the interaction with MHET (Table S3 and Figure S10B). By contrast, in TfCa, certain small residues such as G106, G107, and A108 appear to play an important role in the binding to MHET, in addition to the amino acids neighboring S185 and the aromatic residues F323 and F377 discovered in the crystal structures (Figures 1B,E and S10A). In accordance with the crystal structure analysis, MD simulation results support the conclusion that MHETase has a higher overall binding affinity to MHET than TfCa.

**Substrate Profile of TfCa.** The substrate profile of TfCa was investigated with TPA-based oligo-esters of various lengths, such as MHET, BHET, and 3PET, as well as the ortho-phthalate ester DEP. HPLC-derived product profile allowed us to hypothesize the degradation pathways of longer substrates and estimate the specific activity of TfCa in hydrolyzing various esters at each reaction step (Figure 2).

MHET is the monoester of TPA and EG and also the smallest among all the investigated substrates. The specific activity of MHET hydrolysis by TfCa was 0.024 U/mg[enzyme] as shown in Figure 2A. BHET is the diester of one TPA with two EG. The first hydrolysis of BHET will form MHET and EG, while the second hydrolysis step yields TPA and EG (Figure 2B). The specific activity of TfCa for the first BHET hydrolysis step was found to be much higher (5.12 U/mg[enzyme]) than that of the second hydrolysis step (0.011 U/mg[enzyme]) (Figure 2A,B). Although the second hydrolysis step of BHET is equivalent to the MHET hydrolysis, it revealed an approximately two times lower specific activity than the primary MHET hydrolysis. This can be attributed to a less-preferred binding of MHET in the presence of the competitive substrate BHET, which can be hydrolyzed nearly 500 times faster by TfCa.

Similar to BHET, DEP is a diester of ortho-phthalate and ethanol (Figure 2D). After 1 h of incubation at 50 °C, DEP was not detectable as a result of TfCa-catalyzed hydrolysis. LC−MS analysis suggested that DEP was completely converted to MEP (Figure S11), which can also be monitored as a new peak at a retention time of 11.25 min on HPLC. The specific activity of this primary hydrolysis step is 1.64 U/mg[enzyme], which is 3 times lower than BHET hydrolysis but 82 times higher than MHET hydrolysis. MEP was not further
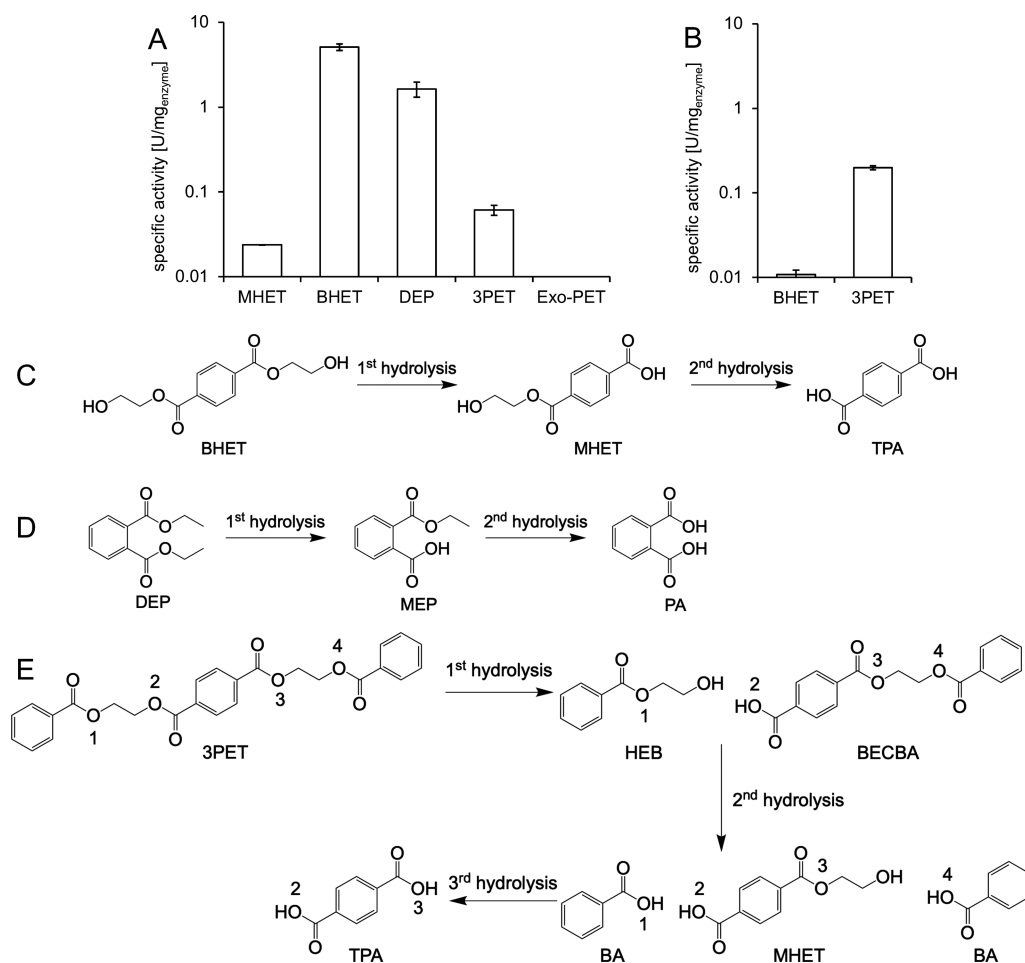
**Figure 2.** TfCa catalyzed hydrolysis of (tere)phthalate esters of various lengths. (A) Specific activity of TfCa for the hydrolysis of the first ester bond in each model substrate. The specific activity is shown on a logarithmic scale. (B) Specific activity of TfCa for the hydrolysis of the second ester bond in 3PET and BHET. The specific activity is shown on a logarithmic scale. Error bars indicate the standard deviations calculated from at least three replicates. Putative degradation pathways for (C) BHET, (D) DEP (TfCa can only catalyze the hydrolysis of DEP to MEP), and (E) 3PET. For simplicity, EG is not shown as a degradation product. Chemical structures and schemes were drawn with ChemDraw 21.0.0.

hydrolyzed to PA, suggesting that it is a less-preferred substrate for TfCa than MHET.

3PET is the longest oligomer investigated in this study with four ester bonds. TfCa-catalyzed hydrolysis of 3PET can yield different product profiles depending on where the first hydrolysis step occurs (Figures S9 and 2E). After 10 min hydrolysis reaction with TfCa at 50 °C, 2-hydroxyethyl-benzoate (HEB) was detected as one product, of which the amount decreases with the reaction duration. Consequently, we suggest a preferential degradation pathway of 3PET, which releases HEB as an intermediate product from 3PET by TfCa. This degradation pattern is similar to that described by Eberl et al.[31] for 3PET hydrolysis catalyzed by a *T. fusca* cutinase. However, the other product from the first hydrolysis step, 4-{[2-(benzoyloxy)ethoxy]-carbonyl} benzoic acid (BECBA) cannot be detected by HPLC. Based on the rate of HEB formation, we determined a specific activity of 0.06 U/mg_enzyme for the first hydrolysis step of 3PET. This is three times higher than for MHET but 85 times and 27 times lower than for BHET and DEP, respectively. The lower specific activity for 3PET is probably due to the size of the substrate. The high specific activity observed for BHET and DEP suggests that (tere)phthalate diesters may have the ideal size for the substrate binding pocket of TfCa. In the second hydrolysis step

of 3PET, both HEB and BECBA are further hydrolyzed. This can be verified by the decreasing concentration of HEB and the increasing amounts of BA and MHET in the samples at the later reaction stage. The estimated specific activity of this reaction step is lower than the first step hydrolysis of 3PET but slightly higher than MHET (Figure 2A). HEB is a monoester comparable to MHET, whereas BECBA is a diester with two aromatic moieties. The markedly lower specific activity observed for BECBA compared to BHET suggests that the additional aromatic ring may hinder the TfCa hydrolysis efficiency. This is consistent with a previous study demonstrating that TfCa can hydrolyze BHET faster than 1,2-ethanediyl bis(4-methylbenzoate).[32] Similar to BECBA, the latter model substrate is a diester with two aromatic moieties and is also commonly used to resemble PET repeating units. The final reaction step of 3PET hydrolysis is MHET hydrolysis, which releases TPA and EG. After a 6 h reaction, MHET was the major product measured by HPLC, followed by BA and TPA (Figure S6).

A previous study has shown that MHETase possesses an exo-PETase activity allowing for the hydrolysis of the terminal ester groups of PET polymers.[16] Accordingly, we tested TfCa for its capacity to hydrolyze PET end groups but were unable to demonstrate its exo-PETase activity (Figures 2A and S7).
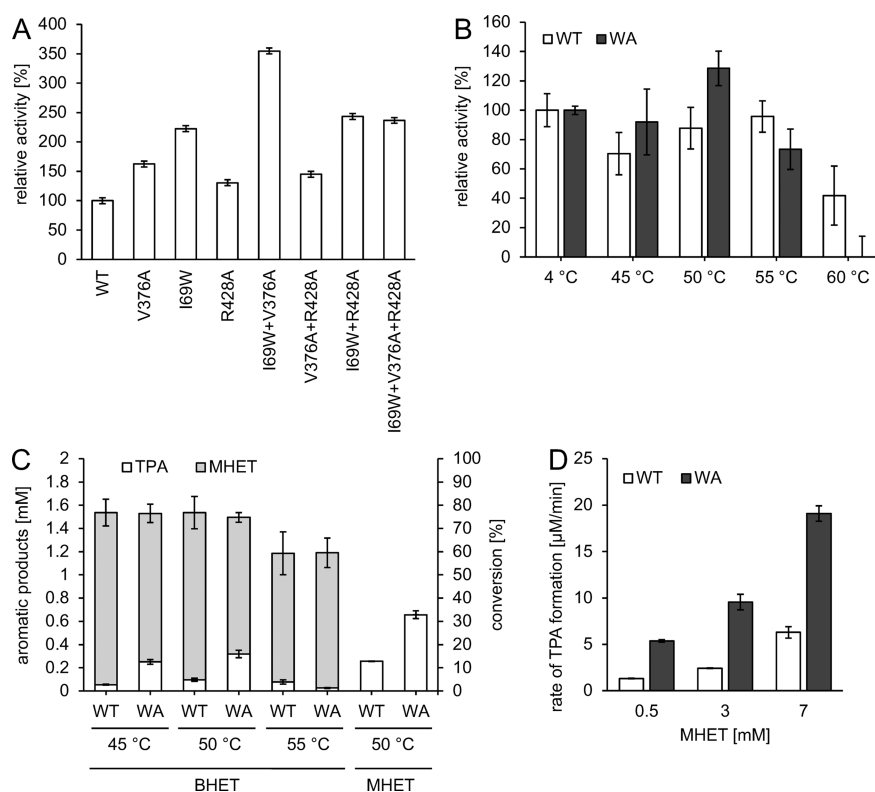
**Figure 3.** Semi-rational enzyme engineering of TfCa and characterization of the most active TfCa^I69W/V376A (WA) mutant. (A) Relative activity of mutants compared to TfCa wt based on the hydrolysis of 2 mM BHET into TPA at 45 °C in 25 mM Tris-buffer (pH 7.5, set at 45 °C). The amount of the degradation product TPA was determined by HPLC analysis. (B) Relative residual activity determined at 25 °C after 1 h incubation at various temperatures. The hydrolytic activity was determined with the model substrate pNPA in 25 mM Tris−HCl buffer (pH 7.5, set at 25 °C). The data determined at 4 °C were used as reference values to define 100% residual activity. (C) 2 mM BHET or MHET were degraded with TfCa wt or TfCa WA at various temperatures in 25 mM Tris−HCl buffer (pH 7.5) for 6 h. The amount of the degradation products MHET and TPA were determined by HPLC. (D) The rates of TPA yield from MHET were determined with 0.55 μM TfCa wt or the variant WA at various substrate concentrations ranging from 0.5 to 7 mM. Reaction supernatants were taken after 30 min of incubation at 50 °C in 25 mM Tris-buffer (pH 7.5, set at 50 °C) and subjected to HPLC analysis. Error bars indicate the standard deviations calculated from at least three replicates.

**Structure-Based Enzyme Engineering of TfCa.** To improve the activity of TfCa on MHET and BHET, amino acid residues within 5 Å of the soaked ligands (Figures 1B,E and S3) were selected for rational engineering. Among the 29 amino acids identified, all alanine, glycine, and proline residues, and those in the catalytic triad as well as the conserved GxSxG motif were excluded from mutagenesis. The remaining 14 residues were individually substituted with alanine (alanine scan). The resulting mutants were first evaluated for BHET hydrolysis activity (Figure S4). Two variants, R428A and V376A, showed ≥1.2-fold higher activity than TfCa wt and were thus selected for further investigations (Figures 3A and S4). R428 and V376 have rather bulky side-chains, which are assumed to affect the substrate binding. As a result, an alanine substitution may possibly provide additional space to accommodate larger substrates like BHET. By contrast, the I69A and M189A variants were completely inactive. These two residues were then subjected to site saturation mutagenesis. The variant I69W was found to be more than twofold more active than that of TfCa wt (Figure 3A), whereas none of the M189 site-saturated mutants was significantly more active with the model substrate pNPA (Figure S5). Based on the complex structures shown in Figures 1 and S3, we hypothesize that the mutation I69W, similar to the residues F323 and F377, may facilitate to interact with the aromatic moiety in the substrate.

All three variants with significantly increased activity, namely, TfCa^R428A, TfCa^V376A, and TfCa^I69W, were combined in all possible variations (Figure 3A). The highest activity was achieved with the mutant TfCa^I69W/V376A, which had a 3.3-fold higher activity on BHET than TfCa wt at 45 °C and is designated as TfCa WA in the following descriptions.

We further investigated the thermostability of TfCa wt and WA. Although TfCa WA has a lower $T_m$ (60.3 °C) than TfCa wt (64.5 °C) (Table S2), its relative residual activities after 1 h incubation at 45, 50, and 55 °C were comparable to those of TfCa wt (Figure 3B). In contrast, TfCa WA became inactive after 1 h at 60 °C whereas TfCa wt had still 40% of its initial activity. Based on these results, we determined the temperature profile of both enzymes for BHET hydrolysis in the temperature range of 45−55 °C (Figure 3C). Although a substrate conversion at a similar level of approximately 80% was obtained with both enzymes after a 6 h reaction at 45 and 50 °C, an overall lower BHET conversion of nearly 60% was determined at 55 °C (Figure 3C). At reaction temperatures up to 50 °C, TfCa WA-catalyzed BHET hydrolysis yielded higher amounts of TPA than TfCa wt. Because the biocatalytic conversion of BHET to TPA requires two ester bond cleavages, this suggested a superior hydrolytic activity of TfCa WA over TfCa wt at up to 50 °C. Although TfCa wt showed a marginally higher yield of TPA from BHET hydrolysis at 55 °C, the considerably lower total substrate
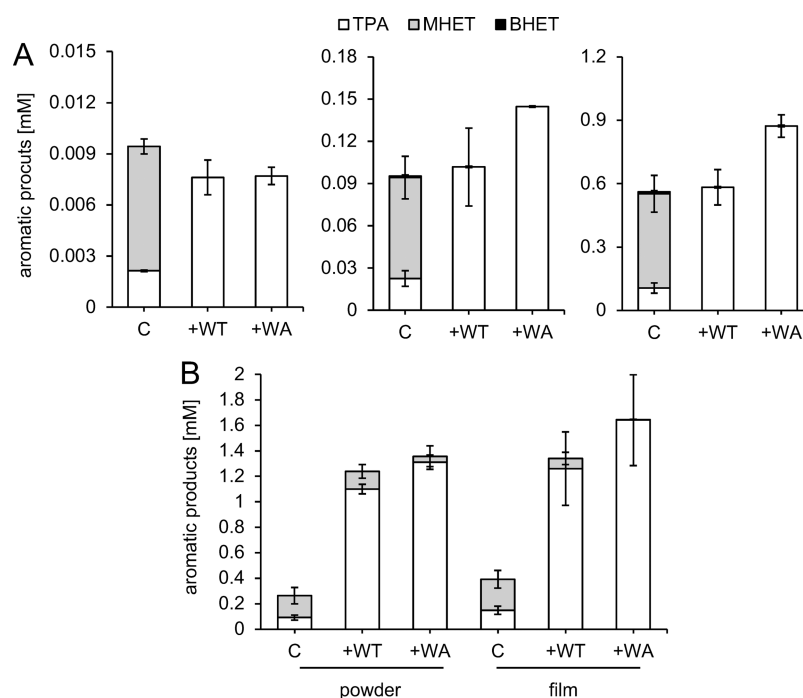
**Figure 4.** Degradation of various PET materials using a dual enzyme system. *Is*PETase PM is present in all samples, C: control without TfCa, wt: with 0.55 $\mu$M TfCa wt, and WA with 0.55 $\mu$M TfCa WA. The experiments were performed in 25 mM Tris−HCl buffer (pH 7.5, set at 45 °C). (A) Varying amounts of PET-NP (left: 2 $\mu$g/mL, middle: 20 $\mu$g/mL, and right: 200 $\mu$g/mL) were degraded using 30 nM of *Is*PETase PM and 0.55 $\mu$M of the indicated TfCa variant. The concentration of aromatic products was determined after 24 h of incubation at 45 °C. Aromatic products detected by HPLC include BHET, MHET, and TPA. (B) Depicted is the same set-up as shown in (A) with high-crystallinity GfPET powder (60 mg/mL) and amorphous PET film (60 mg/mL) as substrates in the presence of 50 nM *Is*PETase PM and 0.55 $\mu$M of the indicated TfCa variant. Error bars indicate the standard deviations calculated from at least three replicates.

conversion levels with both enzymes exclude this temperature as the ideal reaction condition. Thus, 50 °C appeared to be the optimal temperature for BHET hydrolysis by both enzymes. Next, we performed the enzymatic hydrolysis of MHET at 50 °C. At the same substrate concentration of 2 mM, more than twofold TPA was released from MHET compared to BHET with both enzymes. TfCa WA yielded 3.3-fold and 2.6-fold more TPA from the hydrolysis of BHET and MHET than TfCa wt, respectively.

Finally, we compared the rates of TPA release as a result of the enzymatic hydrolysis of MHET at various concentrations ranging from 0.5 to 7 mM (Figure 3D). In agreement with the other experiments described here, TfCa WA hydrolyzed MHET at least three times faster than TfCa wt. The superior activity of TfCa WA is more pronounced at higher substrate concentrations up to 7 mM.

**Degradation of PET Polymers Using a Dual Enzyme System.** We further used free TfCa in a dual enzyme system in combination with a recently published variant of *Is*PETase PM to degrade PET.[25] Based on its temperature profile determined previously,[25] the degradation reaction was performed at 45 °C. At this condition, neither TfCa wt nor TfCa WA can solely degrade PET-NP to release detectable aromatic products (data not shown). First, varying amounts of PET-NP (2, 20, and 200 $\mu$g/mL) were degraded using the dual enzyme system consisting of TfCa and *Is*PETase PM (Figure 4A). When only *Is*PETase PM was present, the main soluble product was MHET independent of the substrate amount used. By adding TfCa wt or its WA variant, TPA was the only detectable product released from PET-NP. With 2 $\mu$g/mL of PET-NP, slightly decreased overall product yields were

obtained when TfCa enzymes are present. At higher substrate concentrations, the overall product yield was up to 1.6-fold higher with the TfCa WA based dual enzyme system than with TfCa wt. The latter enzyme appeared to only convert the MHET and BHET intermediates to TPA but did not further boost the polymer degradation extent.

Next, we used the dual enzyme system to degrade the high-crystalline GfPET powder and the amorphous GfPET film (Figure 4B). These materials are less degradable for PETases than PET-NP because of higher crystallinity and lower relative surface area.[33] Therefore, we used higher substrate and enzyme concentrations to simplify the detection of degradation products. As shown in Figure 4B, the addition of TPA-ester hydrolyzing enzymes has resulted in a markedly increased overall yield of aromatic products with both GfPET film and GfPET powder. When GfPET film was used as the substrate, the overall yield is 3.4- and 4.2-fold higher, respectively, in the presence of TfCa WA and TfCa wt compared to the reaction with solely *Is*PETase PM. Accordingly, the overall product yield improvements with GfPET powder were 4.7- and 5.2-fold with TfCa wt and TfCa WA, respectively. Additionally, as already observed in reactions with PET-NP, the addition of TfCa enzymes eliminated almost completely the MHET fraction in the degradation products. Overall, the TPA yield was increased by 8.3-fold with PET-NP, 14-fold with PET powder, and 11-fold with GfPET film as substrates using the dual enzyme system with TfCa WA as a helper enzyme for *Is*PETase PM.

## ■ DISCUSSION

In this work, we elucidated the apo form as well as ligand-soaked structures of the carboxylesterase TfCa and characterized its enzymatic activity on (tere)phthalate-based oligoesters of various lengths. We found that BHET, an aromatic para-diester, is the most easily hydrolyzable substrate for TfCa. When the diesters are ortho-positioned, like in DEP, or with two aromatic moieties (BECBA), the specific activity becomes lower but is still higher than the hydrolysis of MHET and other monoesters (Figure 2). The aromatic monoester MEP has an ortho-positioned carboxylic acid end group, and it cannot be further hydrolyzed to PA by TfCa. Molecular docking of DEP into the apo form of TfCa suggests that when MEP reenters the active site, it cannot be further hydrolyzed due to its unproductive positioning in the substrate-binding pocket (Figure 5A,B). For the substrate 3PET, we suggest a
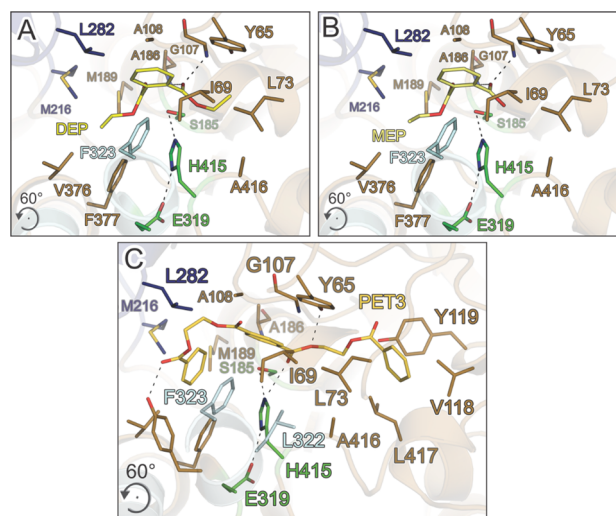


**Figure 5.** Docking results of various substrates to the TfCa apo structure. (A) Positioning of DEP in the active site of TfCa according to docking experiments. The ester closest to S185 will be cleaved, allowing EG and MEP to leave the active site. (B) The most favorable docking pose of MEP in the active site of TfCa is analogous to that after the hydrolysis event of DEP. In this manner, the ester bond in MEP cannot be hydrolyzed by the enzyme. (C) Positioning of 3PET, the largest substrate investigated, in the active site of TfCa supports the suggested degradation pathway. Residues from different domains are shown in brown (TfCa$^{Hyd}$), dark blue (TfCa$^{LidA}$), and cyan (TfCa$^{LidB}$). Ligands are shown as yellow sticks.

degradation pathway based on the analysis of the hydrolysis products. The first hydrolysis step of 3PET forms HEB and BECBA, which is confirmed by docking results shown in Figure 5C. The positioning of the oligo-ester in the substrate-binding pocket of TfCa suggests a preferential hydrolysis of the second ester bond (Figure 2) in 3PET, releasing the products HEB and BECBA. While HEB should leave the binding site earlier in the hydrolysis event, BECBA could presumably bind the same enzyme molecule more easily, allowing it to undergo pseudo-processive hydrolysis to release MHET and BA. This hypothesis is supported by the change of the product profile determined by HPLC during the TfCa-catalyzed hydrolysis of 3PET (Figure S6).

We engineered TfCa toward higher oligo-ester hydrolyzing activity based on crystal structures of TfCa with different

ligands. The mutant TfCa WA possesses a 3.3-fold higher activity in converting BHET to TPA compared to TfCa wt.

We used the variant TfCa WA in a dual enzyme system to depolymerize PET together with a recently published variant of IsPETase.[25] The addition of the carboxylesterase increased the TPA yield in the reaction by up to 14-fold. Similar to MHETase from I. sakaiensis, TfCa alone is not active on PET but can promote the conversion of MHET, which is the major product of enzymatic PET depolymerization by many PET hydrolases,[34] in a dual enzyme system with IsPETase PM. This conversion will not only help to offset the inhibitory effect of MHET on PET hydrolases, but it will furthermore aid in the recovery of extremely pure TPA, which can be directly used for the polymer synthesis.[4,5] In the presence of immobilized TfCa, an increased yield of TPA from PET film has been reported with a dual enzyme system containing the PET hydrolases LC-cutinase or TfCut2.[15] The authors immobilized TfCa using a SulfoLink matrix. This dual enzyme system resulted in an increased overall product yield by 91% for TfCut2 and 104% for LC-cutinase. Using another dual enzyme system containing chimeric I. sakaiensis PETase and MHETase, Knott et al. degraded the amorphous PET film (2−3% crystallinity, Goodfellow, UK) at 30 °C for 96 h using 0.25 mg PETase and 0.5 mg MHETase per gram PET.[12] IsPETase alone produced approximately 0.2 mM TPA at this condition, whereas the addition of free MHETase resulted in a twofold higher TPA yield. The chimeric proteins of MHETase and IsPETase constructed in the same study showed further increased activity by up to seven fold in comparison to the dual free enzyme system.[12] In this study, we used a recently published variant of IsPETase[25] in combination with TfCa wt and WA. Compared to the results reported by Knott et al., we yielded the same amount of TPA from the same substrate (GfPET amorphous film) using 10% IsPETase (0.024 mg/g$_{PET}$) within one-fourth of the reaction time (24 h) at 45 °C.

In general, carboxylesterases such as TfCa are known to exhibit similar functions and contain highly conserved regions. We constructed a phylogenetic tree showing the relationship between the different homologous sequences to TfCa (Figure S8). Some of the strains we found in the phylogenetic tree, for example, Thermobifida alba, Thermobifida halotolerans, and Actinomadura hallensis, contain enzymes known to potentially catalyze the PET polymer degradation.[35−37] Furthermore, the strains Actinomadura rubrobrunea, Actinomadura nitritigenes, and Thermobifida cellulosilytica were mentioned in a phylogenetic study on the characterization and isolation of polyester degrading bacteria.[38] These findings lead to the question of whether polyester depolymerases and oligomer hydrolases co-exist in bacteria. Since both the PETase and the MHETase were found in I. sakaiensis, the emergence of natural dual enzyme systems appears to be a logical conclusion. Additionally, I. sakaiensis was found to metabolize TPA and possess a specific TPA translocation system.[39] However, the lack of a specific transporter machinery for MHET in I. sakaiensis invalidates the assumption that the extracellular PETase and intracellular MHETase can work synergistically during the bacterial assimilation of PET. Similarly, TfCa and TfCut2, the artificially synergistic enzymes in PET depolymerization, are derived from the same species of T. fusca.[15] Unlike I. sakaiensis, the genome of T. fusca[40] does not encode any potential TPA metabolic pathway. Kleeberg et al. have grown a T. fusca strain on mineral salt agar using a TPA-containing aliphatic-aromatic co-polyester as the sole carbon source.[41]

Although the polyesters depolymerized rapidly during the culturing process, only poor bacterial growth was observed. This is in line with the aforementioned genome analysis, which suggests *T. fusca* cannot effectively metabolize PET degradation products, including MHET. As *T. fusca* is extremely unlikely to be able to translocate MHET into the cytosol, similar to *I. sakaiensis*, the role of TfCa in PET depolymerization in the natural environment remains elusive.

The ability of TfCa to degrade the ortho-phthalate ester DEP broadens its substrate specificity. DEP is not only an ortho-phthalate ester but also one of the widely used plasticizers, which are produced annually on a million-ton scale. Plasticizers are added to various polymer materials to alter their properties for easier raw material handling or to meet the application demands required for the end products.[42] However, phthalate-ester-based plasticizers like DEP are known to have endocrine-disrupting, carcinogenic, teratogenic, and mutagenic effects on humans and wildlife.[43] As a result, an efficient decontamination of phthalic esters is a global concern. PA can be assimilated by various microbes and used as a carbon source.[44−46] PA-ring opening enzymes, such as dioxygenases and carboxylesterases, are needed by the PA assimilating species like *Rhodococcus*, *Sphingomonas,* or *Arthrobacter* and others. Nonetheless, our phylogenetic analysis (Figure S8) indicates that these strains are unlikely to express TfCa homologous enzymes. Although the promiscuous hydrolytic activity of TfCa on aromatic oligo-esters in nature is still unknown, the recombinant form of this enzyme has the potential to find ideal application scenarios in the area of environmental biocatalysis and remediation.

In conclusion, the apo and complex crystal structures of TfCa solved in this study shed light on the mechanistic aspects of this enzyme in the hydrolysis of aromatic oligo-esters. These findings allow us to rationally engineer TfCa and apply its most active WA variant in a simple dual enzyme system to relieve product inhibition during enzymatic PET depolymerization. In comparison to previous efforts that employed cross-linked MHETase and *Is*PETase or immobilized TfCa, our simplified dual enzyme system provides a more efficient and less costly solution, which may hold greater promise for industrial-scale applications.[47]

## ■ ASSOCIATED CONTENT

**ⓢ Supporting Information**

The Supporting Information is available free of charge at https://pubs.acs.org/doi/10.1021/acscatal.2c03772.

Materials and methods; data collection of crystal structures; melting temperature of TfCa mutants with increased activity towards BHET; individual contributions of amino acid residues to ligand binding for TfCa and MHETase; ligand binding and unbinding events defined by the catalytic C−O distance for individual protein−ligand complexes with MHET as the ligand; number of snapshots clustered based on the catalytic distance; sequence alignment of TfCa with *p*-nitrobenzyl esterase (pNB-E) and a carboxylesterase; structural alignment of TfCa with *p*-nitrobenzyl esterase and a carboxylesterase; ligand-soaked structure of TfCa with ligand BHET as well as apo form of TfCa docked with DEP and MEP; alanine scan of the substrate binding pocket of TfCa; semi-rational enzyme engineering of TfCa based on the elucidated structures; hydrolysis of

3PET by TfCa over a time course of 6 h; exo-PETase function of TfCa; relation of TfCa to enzymes with similar sequences; putative degradation pathways for 3PET; comparison of residues contributing to the binding of MHET in TfCa and MHETase; confirming MEP as the product of DEP degradation by TfCa; and nucleotide and protein sequence of TfCa wt (PDF)

## ■ AUTHOR INFORMATION

**Corresponding Authors**

**Weidong Liu** − *Tianjin Institute of Industrial Biotechnology, Chinese Academy of Sciences, Tianjin 300308, China; National Technology Innovation Center of Synthetic Biology, Tianjin 300308, China; University of Chinese Academy of Sciences, Beijing 100049, China;* ⓞ orcid.org/0000-0001-7954-7700; Email: liu_wd@tib.cas.cn

**Uwe T. Bornscheuer** − *Department of Biotechnology and Enzyme Catalysis, Institute of Biochemistry, University of Greifswald, 17487 Greifswald, Germany;* ⓞ orcid.org/0000-0003-0685-2696; Email: uwe.bornscheuer@uni-greifswald.de

**Ren Wei** − *Department of Biotechnology and Enzyme Catalysis, Institute of Biochemistry, University of Greifswald, 17487 Greifswald, Germany;* ⓞ orcid.org/0000-0003-3876-1350; Email: ren.wei@uni-greifswald.de

**Authors**

**Gerlis von Haugwitz** − *Department of Biotechnology and Enzyme Catalysis, Institute of Biochemistry, University of Greifswald, 17487 Greifswald, Germany*

**Xu Han** − *Tianjin Institute of Industrial Biotechnology, Chinese Academy of Sciences, Tianjin 300308, China; National Technology Innovation Center of Synthetic Biology, Tianjin 300308, China*

**Lara Pfaff** − *Department of Biotechnology and Enzyme Catalysis, Institute of Biochemistry, University of Greifswald, 17487 Greifswald, Germany;* ⓞ orcid.org/0000-0002-1529-8917

**Qian Li** − *Tianjin Institute of Industrial Biotechnology, Chinese Academy of Sciences, Tianjin 300308, China; National Technology Innovation Center of Synthetic Biology, Tianjin 300308, China*

**Hongli Wei** − *Tianjin Institute of Industrial Biotechnology, Chinese Academy of Sciences, Tianjin 300308, China; National Technology Innovation Center of Synthetic Biology, Tianjin 300308, China*

**Jian Gao** − *Tianjin Institute of Industrial Biotechnology, Chinese Academy of Sciences, Tianjin 300308, China; National Technology Innovation Center of Synthetic Biology, Tianjin 300308, China*

**Karen Methling** − *Department of Cellular Biochemistry and Metabolomics, Institute of Biochemistry, University of Greifswald, 17487 Greifswald, Germany*

**Yufei Ao** − *Department of Biotechnology and Enzyme Catalysis, Institute of Biochemistry, University of Greifswald, 17487 Greifswald, Germany; University of Chinese Academy of Sciences, Beijing 100049, China*

**Yannik Brack** − *Department of Biotechnology and Enzyme Catalysis, Institute of Biochemistry, University of Greifswald, 17487 Greifswald, Germany*

**Jan Mican** − *Loschmidt Laboratories, Department of Experimental Biology and RECETOX, Faculty of Science, Masaryk University, 625 00 Brno, Czech Republic;*

*International Clinical Research Center, St. Anne's University Hospital, 656 91 Brno, Czech Republic;* ⓘ orcid.org/0000-0002-8877-163X

**Christian G. Feiler** − *Macromolecular Crystallography, Helmholtz-Zentrum Berlin, 12489 Berlin, Germany*

**Manfred S. Weiss** − *Macromolecular Crystallography, Helmholtz-Zentrum Berlin, 12489 Berlin, Germany*

**David Bednar** − *Loschmidt Laboratories, Department of Experimental Biology and RECETOX, Faculty of Science, Masaryk University, 625 00 Brno, Czech Republic; International Clinical Research Center, St. Anne's University Hospital, 656 91 Brno, Czech Republic*

**Gottfried J. Palm** − *Department of Synthetic and Structural Biochemistry, Institute of Biochemistry, University of Greifswald, 17487 Greifswald, Germany;* ⓘ orcid.org/0000-0003-0329-0413

**Michael Lalk** − *Department of Cellular Biochemistry and Metabolomics, Institute of Biochemistry, University of Greifswald, 17487 Greifswald, Germany*

**Michael Lammers** − *Department of Synthetic and Structural Biochemistry, Institute of Biochemistry, University of Greifswald, 17487 Greifswald, Germany*

**Jiri Damborsky** − *Loschmidt Laboratories, Department of Experimental Biology and RECETOX, Faculty of Science, Masaryk University, 625 00 Brno, Czech Republic; International Clinical Research Center, St. Anne's University Hospital, 656 91 Brno, Czech Republic*

**Gert Weber** − *Macromolecular Crystallography, Helmholtz-Zentrum Berlin, 12489 Berlin, Germany;* ⓘ orcid.org/0000-0003-3624-1060

Complete contact information is available at:
https://pubs.acs.org/10.1021/acscatal.2c03772

## Author Contributions

Conceptualization, R.W., W.L., and U.T.B.; protein crystallographic studies, J.G., X.H., C.G.F., Q.L., G.J.P., M.L., and W.L.; computational simulations, G.W., J.M., D.B., J.D., and W.L.; protein engineering and characterization, G.H.; substrate generation and characterization, Y.A. and L.P.; product identification, G.H., K.M., M.L., and R.W.; generation of the phylogenetic tree, Y.B.; writing—original draft, G.H., J.M., W.L., and R.W.; writing, review and editing, all authors; supervision and funding acquisition, J.D., W.L., U.T.B., and R.W.

## Notes

The authors declare no competing financial interest.

## ◾ ABBREVIATIONS

| | |
|---|---|
| BA | benzoic acid |
| BECBA | 4-{[2-(benzoyloxy)ethoxy]-carbonyl} benzoic acid |
| BHET | bis(2-hydroxyethyl) terephthalate |
| DEP | diethyl phthalate |
| DMSO | dimethyl sulfoxide |
| DSF | differential scanning fluorimetry |
| EG | ethylene glycol |
| GfPET | amorphous PET film purchased from Goodfellow Ltd. |
| HEB | 2-hydroxyethyl-benzoate |
| HPLC | high-performance liquid chromatography |
| IPTG | isopropyl $\beta$-D-thiogalactopyranoside |
| *Is*PETase PM | a variant of PETase from *Ideonella sakaiensis* |
| LC−MS | liquid chromatography coupled with mass spectrometry |
| MEP | monoethyl phthalate |
| MD | molecular dynamics |
| MHET | mono(2-hydroxyethyl) terephthalate |
| MHETA | 4-[(2-hydroxyethyl) carbamoyl] benzoic acid |
| MR | molecular replacement |
| Ni-NTA | $Ni^{2+}$-nitrilotriacetic acid |
| $OD_{600}$ | optical density measured at 600 nm |
| NP | nanoparticle |
| PA | phthalic acid |
| PET | polyethylene terephthalate |
| PETase | PET hydrolase |
| pNPA | para-nitrophenyl acetate |
| *p*-NP-E | *p*-nitrobenzyl esterase |
| *T. fusca* | *Thermobifida fusca* |
| TfCa | carboxylesterase from *T. fusca* |
| $T_g$ | glass transition temperature |
| $T_m$ | melting temperature |
| TPA | terephthalate |
| WA | TfCa variant[I69W/V376A] |
| 3PET | bis[2-(benzoyloxy)ethyl] terephthalate |

## ◾ REFERENCES

(1) Wei, R.; Tiso, T.; Bertling, J.; O'Connor, K.; Blank, L. M.; Bornscheuer, U. T. Possibilities and limitations of biotechnological plastic degradation and recycling. *Nat. Catal.* **2020**, 3, 867−871.

(2) Müller, R.-J.; Schrader, H.; Profe, J.; Dresler, K.; Deckwer, W.-D. Enzymatic degradation of poly(ethylene terephthalate): Rapid hydrolyse using a hydrolase from *T. fusca*. *Macromol. Rapid Commun.* **2005**, 26, 1400−1405.

(3) Lu, H.; Diaz, D. J.; Czarnecki, N. J.; Zhu, C.; Kim, W.; Shroff, R.; Acosta, D. J.; Alexander, B. R.; Cole, H. O.; Zhang, Y.; Lynd, N. A.;

Ellington, A. D.; Alper, H. S. Machine learning-aided engineering of hydrolases for PET depolymerization. *Nature* **2022**, *604*, 662–667.

(4) Wei, R.; von Haugwitz, G.; Pfaff, L.; Mican, J.; Badenhorst, C. P. S.; Liu, W.; Weber, G.; Austin, H. P.; Bednar, D.; Damborsky, J.; Bornscheuer, U. T. Mechanism-based design of efficient PET hydrolases. *ACS Catal.* **2022**, *12*, 3382–3396.

(5) Tournier, V.; Topham, C. M.; Gilles, A.; David, B.; Folgoas, C.; Moya-Leclair, E.; Kamionka, E.; Desrousseaux, M.-L.; Texier, H.; Gavalda, S.; Cot, M.; Guémard, E.; Dalibey, M.; Nomme, J.; Cioci, G.; Barbe, S.; Chateau, M.; André, I.; Duquesne, S.; Marty, A. An engineered PET depolymerase to break down and recycle plastic bottles. *Nature* **2020**, *580*, 216–219.

(6) Wei, R.; Zimmermann, W. Microbial enzymes for the recycling of recalcitrant petroleum-based plastics: how far are we? *Microb. Biotechnol.* **2017**, *10*, 1308–1322.

(7) Barth, M.; Oeser, T.; Wei, R.; Then, J.; Schmidt, J.; Zimmermann, W. Effect of hydrolysis products on the enzymatic degradation of polyethylene terephthalate nanoparticles by a polyester Hydrolase from *Thermobifida fusca. Biochem. Eng. J.* **2015**, *93*, 222–228.

(8) Barth, M.; Wei, R.; Oeser, T.; Then, J.; Schmidt, J.; Wohlgemuth, F.; Zimmermann, W. Enzymatic hydrolysis of poly-ethylene terephthalate films in an ultrafiltration membrane reactor. *J. Membr. Sci.* **2015**, *494*, 182–187.

(9) Wei, R.; Oeser, T.; Schmidt, J.; Meier, R.; Barth, M.; Then, J.; Zimmermann, W. Engineered bacterial polyester hydrolases efficiently degrade polyethylene terephthalate due to relieved product inhibition. *Biotechnol. Bioeng.* **2016**, *113*, 1658–1665.

(10) Yoshida, S.; Hiraga, K.; Takehana, T.; Taniguchi, I.; Yamaji, H.; Maeda, Y.; Toyohara, K.; Miyamoto, K.; Kimura, Y.; Oda, K. A bacterium that degrades and assimilates poly(ethylene terephthalate). *Science* **2016**, *351*, 1196–1199.

(11) Palm, G. J.; Reisky, L.; Böttcher, D.; Müller, H.; Michels, E. A. P.; Walczak, M. C.; Berndt, L.; Weiss, M. S.; Bornscheuer, U. T.; Weber, G. Structure of the plastic-degrading *Ideonella sakaiensis* MHETase bound to a substrate. *Nat. Commun.* **2019**, *10*, 1717.

(12) Knott, B. C.; Erickson, E.; Allen, M. D.; Gado, J. E.; Graham, R.; Kearns, F. L.; Pardo, I.; Topuzlu, E.; Anderson, J. J.; Austin, H. P.; Dominick, G.; Johnson, C. W.; Rorrer, N. A.; Szostkiewicz, C. J.; Copié, V.; Payne, C. M.; Woodcock, H. L.; Donohoe, B. S.; Beckham, G. T.; McGeehan, J. E. Characterization and engineering of a two-enzyme system for plastics depolymerization. *Proc. Natl. Acad. Sci. U. S. A.* **2020**, *117*, 25476–25485.

(13) Billig, S.; Oeser, T.; Birkemeyer, C.; Zimmermann, W. Hydrolysis of cyclic poly(ethylene terephthalate) trimers by a carboxylesterase from *Thermobifida fusca* KW3. *Appl. Microbiol. Biotechnol.* **2010**, *87*, 1753–1764.

(14) Oeser, T.; Wei, R.; Baumgarten, T.; Billig, S.; Föllner, C.; Zimmermann, W. High level expression of a hydrophobic poly-(ethylene terephthalate)-hydrolyzing carboxylesterase from *Thermobifida fusca* KW3 in *Escherichia coli* BL21(DE3). *J. Biotechnol.* **2010**, *146*, 100–104.

(15) Barth, M.; Honak, A.; Oeser, T.; Wei, R.; Belisário-Ferrari, M. R.; Then, J.; Schmidt, J.; Zimmermann, W. A dual enzyme system composed of a polyester hydrolase and a carboxylesterase enhances the biocatalytic degradation of polyethylene terephthalate films. *Biotechnol. J.* **2016**, *11*, 1082–1087.

(16) Sagong, H.-Y.; Seo, H.; Kim, T.; Son, H. F.; Joo, S.; Lee, S. H.; Kim, S.; Woo, J.-S.; Hwang, S. Y.; Kim, K.-J. Decomposition of the PET film by MHETase using exo-PETase function. *ACS Catal.* **2020**, *10*, 4805–4812.

(17) Pfaff, L.; Breite, D.; Badenhorst, C. P. S.; Bornscheuer, U.; Wei, R. Fluorimetric high-throughput screening method for polyester hydrolase activity using polyethylene terephthalate nanoparticles. *Methods Enzymol.* **2021**, *648*, 253–270.

(18) Fischer-Colbrie, G.; Heumann, S.; Liebminger, S.; Almansa, E.; Cavaco-Paulo, A.; Guebitz, G. M. New enzymes with potential for PET surface modification. *Biocatal. Biotransform.* **2004**, *22*, 341–346.

(19) Mueller, U.; Förster, R.; Hellmig, M.; Huschmann, F. U.; Kastner, A.; Malecki, P.; Pühringer, S.; Röwer, M.; Sparta, K.; Steffien, M.; Ühlein, M.; Wilk, P.; Weiss, M. S. The macromolecular crystallography beamlines at BESSY II of the Helmholtz-Zentrum Berlin: Current status and perspectives. *Eur. Phys. J. Plus* **2015**, *130*, 141.

(20) McCoy, A. J.; Grosse-Kunstleve, R. W.; Adams, P. D.; Winn, M. D.; Storoni, L. C.; Read, R. J. Phaser crystallographic software. *J. Appl. Crystallogr.* **2007**, *40*, 658–674.

(21) Liebschner, D.; Afonine, P. V.; Baker, M. L.; Bunkóczi, G.; Chen, V. B.; Croll, T. I.; Hintze, B.; Hung, L.-W.; Jain, S.; McCoy, A. J.; Moriarty, N. W.; Oeffner, R. D.; Poon, B. K.; Prisant, M. G.; Read, R. J.; Richardson, J. S.; Richardson, D. C.; Sammito, M. D.; Sobolev, O. V.; Stockwell, D. H.; Terwilliger, T. C.; Urzhumtsev, A. G.; Videau, L. L.; Williams, C. J.; Adams, P. D. Macromolecular structure determination using X-rays, neutrons and electrons: recent developments in Phenix. *Acta Crystallogr. D Struct. Biol.* **2019**, *75*, 861–877.

(22) Afonine, P. V.; Grosse-Kunstleve, R. W.; Echols, N.; Headd, J. J.; Moriarty, N. W.; Mustyakimov, M.; Terwilliger, T. C.; Urzhumtsev, A.; Zwart, P. H.; Adams, P. D. Towards automated crystallographic structure refinement with phenix.refine. *Acta Crystallogr. D Biol. Crystallogr.* **2012**, *68*, 352–367.

(23) Emsley, P.; Cowtan, K. Coot: model-building tools for molecular graphics. *Acta Crystallogr. D Biol. Crystallogr.* **2004**, *60*, 2126–2132.

(24) Brünger, A. T. Assessment of phase accuracy by cross validation: the free R value. Methods and applications. *Acta Crystallogr. D Biol. Crystallogr.* **1993**, *49*, 24–36.

(25) Brott, S.; Pfaff, L.; Schuricht, J.; Schwarz, J.-N.; Böttcher, D.; Badenhorst, C. P. S.; Wei, R.; Bornscheuer, U. T. Engineering and evaluation of thermostable *Is*PETase variants for PET degradation. *Eng. Life Sci.* **2022**, *22*, 192–203.

(26) Trott, O.; Olson, A. J. AutoDock Vina: improving the speed and accuracy of docking with a new scoring function, efficient optimization, and multithreading. *J. Comput. Chem.* **2010**, *31*, 455–461.

(27) Berman, H. M.; Westbrook, J.; Feng, Z.; Gilliland, G.; Bhat, T. N.; Weissig, H.; Shindyalov, I. N.; Bourne, P. E. The Protein Data Bank. *Nucleic Acids Res.* **2000**, *28*, 235–242.

(28) Miller, B. R.; McGee, T. D.; Swails, J. M.; Homeyer, N.; Gohlke, H.; Roitberg, A. E. MMPBSA.py: An efficient program for end-state free energy calculations. *J. Chem. Theory Comput.* **2012**, *8*, 3314–3321.

(29) Genheden, S.; Ryde, U. The MM/PBSA and MM/GBSA methods to estimate ligand-binding affinities. *Expert Opin. Drug Discov.* **2015**, *10*, 449–461.

(30) Weiser, J.; Shenkin, P. S.; Still, W. C. Approximate atomic surfaces from linear combinations of pairwise overlaps (LCPO). *J. Comput. Chem.* **1999**, *20*, 217–230.

(31) Eberl, A.; Heumann, S.; Brückner, T.; Araujo, R.; Cavaco-Paulo, A.; Kaufmann, F.; Kroutil, W.; Guebitz, G. M. Enzymatic surface hydrolysis of poly(ethylene terephthalate) and bis-(benzoyloxyethyl) terephthalate by lipase and cutinase in the presence of surface active molecules. *J. Biotechnol.* **2009**, *143*, 207–212.

(32) Belisário-Ferrari, M. R.; Wei, R.; Schneider, T.; Honak, A.; Zimmermann, W. Fast turbidimetric assay for analyzing the enzymatic hydrolysis of polyethylene terephthalate model substrates. *Biotechnol. J.* **2019**, *14*, No. 1800272.

(33) Vogel, K.; Wei, R.; Pfaff, L.; Breite, D.; Al-Fathi, H.; Ortmann, C.; Estrela-Lopis, I.; Venus, T.; Schulze, A.; Harms, H.; Bornscheuer, U. T.; Maskow, T. Enzymatic degradation of polyethylene terephthalate nanoplastics analyzed in real time by isothermal titration calorimetry. *Sci. Total Environ.* **2021**, *773*, No. 145111.

(34) Pfaff, L.; Gao, J.; Li, Z.; Jäckering, A.; Weber, G.; Mican, J.; Chen, Y.; Dong, W.; Han, X.; Feiler, C. G.; Ao, Y.-F.; Badenhorst, C. P. S.; Bednar, D.; Palm, G. J.; Lammers, M.; Damborsky, J.; Strodel, B.; Liu, W.; Bornscheuer, U. T.; Wei, R. Multiple substrate binding mode-guided engineering of a thermophilic PET hydrolase. *ACS Catal.* **2022**, *12*, 9790–9800.

(35) Ribitsch, D.; Herrero Acero, E.; Greimel, K.; Dellacher, A.; Zitzenbacher, S.; Marold, A.; Rodriguez, R. D.; Steinkellner, G.; Gruber, K.; Schwab, H.; Guebitz, G. M. A New esterase from *Thermobifida halotolerans* hydrolyses polyethylene terephthalate (PET) and polylactic acid (PLA). *Polymer* **2012**, *4*, 617−629.

(36) Samak, N. A.; Jia, Y.; Sharshar, M. M.; Mu, T.; Yang, M.; Peh, S.; Xing, J. Recent advances in biocatalysts engineering for polyethylene terephthalate plastic waste green recycling. *Environ. Int.* **2020**, *145*, No. 106144.

(37) Sonnendecker, C.; Oeser, J.; Richter, P. K.; Hille, P.; Zhao, Z.; Fischer, C.; Lippold, H.; Blázquez-Sánchez, P.; Engelberger, F.; Ramírez-Sarmiento, C. A.; Oeser, T.; Lihanova, Y.; Frank, R.; Jahnke, H.-G.; Billig, S.; Abel, B.; Sträter, N.; Matysik, J.; Zimmermann, W. Low carbon footprint recycling of post-consumer PET plastic with a metagenomic polyester hydrolase. *ChemSusChem* **2022**, *15*, No. e202101062.

(38) Sriyapai, P.; Chansiri, K.; Sriyapai, T. Isolation and character-ization of polyester-based plastics-degrading bacteria from compost soils. *Microbiology* **2018**, *87*, 290−300.

(39) Gautom, T.; Dheeman, D.; Levy, C.; Butterfield, T.; Alvarez Gonzalez, G.; Le Roy, P.; Caiger, L.; Fisher, K.; Johannissen, L.; Dixon, N. Structural basis of terephthalate recognition by solute binding protein TphC. *Nat. Commun.* **2021**, *12*, 6244.

(40) Lykidis, A.; Mavromatis, K.; Ivanova, N.; Anderson, I.; Land, M.; DiBartolo, G.; Martinez, M.; Lapidus, A.; Lucas, S.; Copeland, A.; Richardson, P.; Wilson, D. B.; Kyrpides, N. Genome sequence and analysis of the soil cellulolytic actinomycete *Thermobifida fusca* YX. *J. Bacteriol.* **2007**, *189*, 2477−2486.

(41) Kleeberg, I.; Hetz, C.; Kroppenstedt, R. M.; Müller, R.-J.; Deckwer, W.-D. Biodegradation of aliphatic-aromatic copolyesters by *Thermomonospora fusca* and other thermophilic compost isolates. *Appl. Environ. Microbiol.* **1998**, *64*, 1731−1735.

(42) Giam, C. S.; Atlas, E.; Powers, M. A.; Leonard, J. E. Phthalic acid esters. In *Anthropogenic Compounds*; Springer: Berlin, Heidelberg, 1984; pp. 67−142.

(43) Baloyi, N. D.; Tekere, M.; Maphangwa, K. W.; Masindi, V. Insights into the prevalence and impacts of phthalate esters in aquatic ecosystems. *Front. Environ. Sci.* **2021**, *9*, No. 684190.

(44) Boll, M.; Geiger, R.; Junghare, M.; Schink, B. Microbial degradation of phthalates: biochemistry and environmental implica-tions. *Environ. Microbiol. Rep.* **2020**, *12*, 3−15.

(45) Gao, D.-W.; Wen, Z.-D. Phthalate esters in the environment: A critical review of their occurrence, biodegradation, and removal during wastewater treatment processes. *Sci. Total Environ.* **2016**, *541*, 986−1001.

(46) Vamsee-Krishna, C.; Phale, P. S. Bacterial degradation of phthalate isomers and their esters. *Indian J. Microbiol.* **2008**, *48*, 19−34.

(47) Singh, A.; Rorrer, N. A.; Nicholson, S. R.; Erickson, E.; DesVeaux, J. S.; Avelino, A. F. T.; Lamers, P.; Bhatt, A.; Zhang, Y.; Avery, G.; Tao, L.; Pickford, A. R.; Carpenter, A. C.; McGeehan, J. E.; Beckham, G. T. Techno-economic, life-cycle, and socioeconomic impact analysis of enzymatic recycling of poly(ethylene terephtha-late). *Joule* **2021**, *5*, 2479−2503.